

HOKKAIDO UNIVERSITY

Title	Activation cross sections of longer-lived radionuclides produced in germanium by alpha particle irradiation
Author(s)	Takacs, S.; Takacs, M. P.; Ditroi, F. et al.
Citation	Nuclear Instruments and Methods in Physics Research Section B : Beam Interactions with Materials and Atoms, 383, 213-226 https://doi.org/10.1016/j.nimb.2016.07.015
Issue Date	2016-09-15
Doc URL	https://hdl.handle.net/2115/71220
Rights	c2016, Elsevier. Licensed under the Creative Commons Attribution-NonCommercial-NoDerivatives 4.0 International http://creativecommons.org/licenses/by-nc-nd/4.0/
Rights(URL)	https://creativecommons.org/licenses/by-nc-nd/4.0/
Type	journal article
File Information	NIMPR B383 213-226.pdf



Hokkaido University Collection of Scholarly and Academic Papers : HUSCAP

Activation cross sections of longer-lived radionuclides produced in germanium by alpha particle irradiation

S. Takács[1,*], M.P. Takács[1,†], F. Ditrói[1], M. Aikawa[2], H. Haba[3], Y. Komori[3]

[1] Institute for Nuclear Research, Hungarian Academy of Sciences, Atomki, 4026 Debrecen, Hungary
[2] Faculty of Science, Hokkaido University, Sapporo 060-0810, Japan
[3] Nishina Center for Accelerator-Based Science, RIKEN, Wako, Saitama 351-0198, Japan

Abstract

The cross sections of alpha particles induced nuclear reactions on natural germanium were investigated by using the standard stacked foil target technique, the activation method and high resolution gamma spectrometry. Targets with thickness of about 1 μm were prepared from natural Ge by vacuum evaporation onto 25 μm thick polyimide (Kapton) backing foils. Stacks were composed of Kapton-Ge-Ge-Kapton sandwich target foils and additional titanium monitor foils with nominal thickness of 11 micrometers to monitor the beam parameters using the $^{nat}Ti(\alpha,x)^{51}Cr$ reaction. The irradiations were done with E_α = 20.7 and E_α = 51.25 MeV, I_α = 50 nA alpha particle beams for about 1 hour. Direct or cumulative activation cross sections were determined for production of the $^{72,73,75}Se$, $^{71,72,74,76,78}As$, and ^{69}Ge radionuclides. The obtained experimental cross sections were compared to the results of theoretical calculations taken from the TENDL data library based on the TALYS computer code. A comparison was made with available experimental data measured earlier. Thick target yields were deduced from the experimental cross sections and compared with the data published before.

Keywords: alpha particle irradiation, natural germanium target, cross sections, $^{72,73,75}Se$, $^{71,72,74,76,78}As$ and ^{69}Ge excitation functions, TENDL comparison.

1. Introduction

As a part of the project focused on systematic measurement of the charged particle induced nuclear reaction cross sections going on in Atomki for several years now, alpha particle induced reactions on germanium were investigated up to E_α = 51.25 MeV. In the interaction of Ge target material and alpha particles, isotopes of Se, As, Ge and Ga can be considered as primary reaction products. Additional reaction channels are also possible with lower probability producing Cu isotopes. Proton and deuteron bombardment of Ge have been already investigated [1] [2] [3] [4], [5], [6]. For alpha particle induced reactions the available data are limited and show large discrepancies [7], [8], [9], [10], [11], [12]. The aim of our study was to measure cross section data in well-controlled experimental circumstances and to try to resolve the discrepancies among the available data sets. The cross sections were measured on Ge target with natural isotopic composition in this work. The presented data are linear combinations of the cross section values of the reactions, which take place on stable isotopes of germanium with different mass number. The weighting factors are the isotopic abundances. Naturally occurring Ge has five stable isotopes: ^{70}Ge (20.57%), ^{72}Ge (27.45%), ^{73}Ge (7.75%), ^{74}Ge (36.50%) and ^{76}Ge (7.73%) [13].
The excitation functions of the alpha particle induced reactions on natural germanium leading to the longer-lived γ-emitting radionuclides are presented here. The arsenic radioisotopes ^{71}As,

* Corresponding author: email: stakacs@atomki.hu
† *Current Address: Helmholtz-Zentrum Dresden-Rossendorf (HZDR), D-01328 Dresden, Germany*

^{72}As and ^{74}As have decay characteristics that make them suitable for use in PET investigations [14, 15, 16], while ^{73}As and ^{74}As are suitable for tracing environmental processes [17], due to their longer half-lives. The ^{76}As could potentially be used for tumour therapy [18] due to the longer half-life, the higher dose rate and the suitable β^--particle energy. The long-lived γ-emitting ^{73}Se and ^{75}Se can be also potentially used in medical applications because Se is one of essential bio-trace elements in the body.
As part of the effort to develop theoretical models and computer codes to describe the probability of different nuclear reactions as a function of the bombarding particle energy, the deduced experimental cross section data may contribute to further development of the theoretical models and their computer codes.
The new experimental data were compared with the available, earlier published data, and with the results of recent calculations performed by using the TALYS code for the investigated radionuclides. Physical thick target yields were calculated from the measured cross sections and were compared to the available experimental yields.

2. Experimental

2.1 Target preparation

The germanium targets were prepared by vacuum evaporation. A 25 μm thin polyimide (Kapton) foil was used as target backing. The evaporation was done from a direct current resistive heated open tungsten boat. The cooled Kapton foils of d = 14 mm in diameter were placed about 20 cm from the source of the evaporated germanium. A circular mask with diameter of 11 mm was applied to determine the size of the evaporated Ge spot. The 20 cm distance assured production of a quasi-uniform deposited germanium layer. Each Kapton backing was numbered and its weight was measured before and after the evaporation, thus the amount of the deposited germanium was determined. From the mass of the deposited germanium and area of the deposited spot an average thickness of 1 μm thick Ge layer was calculated. The prepared Kapton-Ge samples were sorted by the amount of deposited Ge mass, then Kapton-Ge-Ge-Kapton sandwich targets were created by grouping always the lowest and highest Ge mass samples together. This way 35 sandwich Ge targets were prepared. Four complete stacked targets were assembled using the Ge sandwich foils interleaved with some Ti foils (10.9 μm thick, Goodfellow, 99.99%) for monitoring the beam intensity and to moderate the beam energy. One stack was irradiated at E_α = 51.25 MeV in RIKEN at the AVF cyclotron beam line, the other three at E_α = 20.7 MeV primary alpha particle beam at the Atomki MGC-20E cyclotron. The sandwich target has the advantage that no recoil corrections needed to be applied since the Kapton backing served as a catcher foil for the possible recoiled reaction products.

2.2 Irradiation

The irradiations were done in a specially designed air cooled, Faraday cup like vacuum chamber equipped with a long collimator, assuring a negligible small solid angle for the secondary electrons escape. Four irradiations were performed. The irradiation at RIKEN took place at an external beam line of the AVF cyclotron. The initial beam energy was set to be E_α = 51.25 MeV which was confirmed by time-of-flight energy measurement [19, 20]. The beam current was kept constant at about I_α = 50 nA during the 1.0 h irradiation time. The collected charge was recorded every minute to check the beam stability. The irradiated stack contained

23 Kapton-Ge-Ge-Kapton sandwich targets interleaved with Ti monitor foils (10.9 μm thick, Goodfellow, 99.99%).
The three E_α = 20.7 MeV irradiations took place at an external beam line of the MGC20E cyclotron of Atomki. Each stack contained 4 Ge sandwich target foils and different number of Ti foils to monitor the beam parameters and to shift the mean energy inside the Ge sandwich targets in order to cover the available energy region more evenly. Another stack containing only Ti monitor foils was irradiated with the same cyclotron tuning parameters in order to double check the beam parameters. Each irradiation lasted 1 h and the beam intensity was kept at I_α = 50 nA. Comparison of the recommended cross sections for the $^{nat}Ti(\alpha,x)^{51}Cr$ monitor reaction and the recoil corrected experimental values deduced in our study can be seen in Fig. 1. The experimental cross section points and the recommended data [21] are in good agreement, indicating that the deduced beam parameters, the energy scale calculation, and the data deduction method are correct.

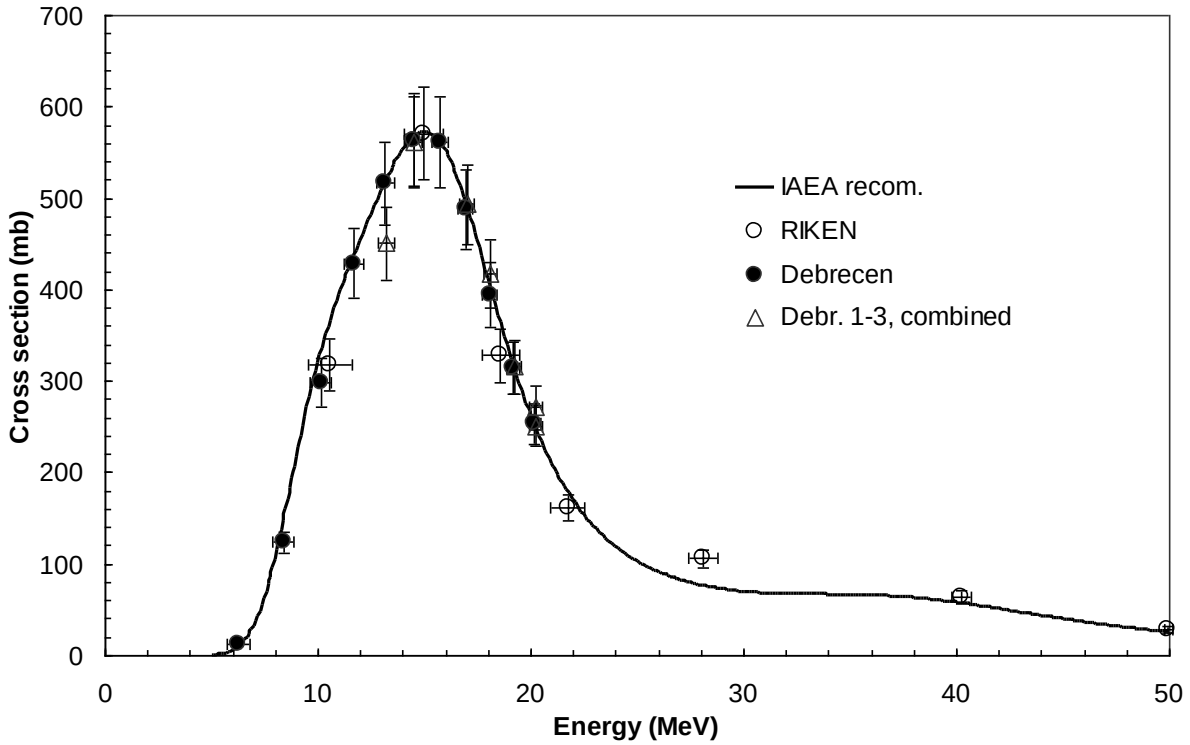

Figure 1. Comparison of the recommended excitation function of the $^{nat}Ti(\alpha,x)^{51}Cr$ reaction [21] and the experimental cross section data points deduced in these experiments. The open circle represents the experiment in RIKEN, the full dot represents the stack in Atomki containing only Ti foils, and the open triangle represents the combined three experiments in Atomki with Ge targets.

2.3. Activity measurements

After irradiation and applying a short cooling time, the activated Ge targets and the Ti monitor foils were separated from the stacks and enclosed individually in small plastic bags for gamma spectroscopic measurement. The activity of the produced radionuclides in each target and monitor foil was assessed with no chemical separation using high-resolution, HPGe based gamma-ray spectrometry. The detectors were manufactured by Ortec Company in RIKEN and by Canberra Company in Atomki. Gamma-spectra were acquired at different

sample-detector distances to keep the dead time low. At least three series of measurements were performed for the Ge targets to follow the decay of the produced radionuclides. The first series started about 1–6 h cooling time after the end of bombardment (EOB), and each measurement lasted about 10 minutes. The second series of measurements were performed with an average cooling time of 15 h after EOB and the applied measuring times were between 0.3 and 2 hours. The third series were started after minimum 100 hours of cooling time. The activity of the Ti monitor foils was assessed after a week of cooling time. To keep the pileup effect and the dead time of the electronics low, the detector sample distance was set between 25 and 5 cm. Spectra measured in one series were acquired at the same distance. The typical dead time value was about 7% for the first series of measurements and ≤ 1% for the late measurements.
The geometry dependent detector efficiency was determined for the used sample-detector distances by using standard activity calibrated gamma-sources. The net photo-peak area in the spectra was calculated using the fitting algorithm included in the acquisition software packages. Separation of overlapping complex peaks was done by the FORGAMMA [22], an interactive peak analysis code.

2.4. Cross section determination

The cross section was calculated from the measured activity of the target foils using the activation and decay laws, the irradiation parameters, decay data and necessary corrections. The following general approximations were considered in data analysis

- Constant beam current during the irradiation
- Thin target foil in which the energy degradation of the bombarding particles can be approximated by a linear function
- The energy dependent cross section within one irradiated foil can be approximated by a linear function

Accepting the above three estimations the deduced cross section value can be assigned to the mid-energy point of the target foils. The mid energy point for a target foil was calculated as the mathematical average of the incoming and outgoing energy of the bombarding particles. The energy loss of the bombarding particles in the stacked target was estimated by using the STOPPING computer code based on the polynomial approximation method of Andersen and Ziegler [23]. The energy scale provided by the energy loss calculation and the direct measured number of incident particles per unit time were compared with the deduced from the re-measured recoil corrected excitation function of the ^{nat}Ti(α,x)^{51}Cr monitor reaction. The recommended cross section data for the ^{nat}Ti(α,x)^{51}Cr monitor reaction were taken from the upgraded web version of the IAEA database [21]. The direct measurement provided an average beam current of 49 nA, which was 3.5% higher than the one deduced by using the monitor reaction. This can be considered as a good agreement. The recommended and experimental excitation functions of the monitor reaction are compared in Fig 1. The overall agreement between the measured and recommended data validates the energy degradation calculation throughout the stack, the beam intensity measurements and cross section deduction method.
The corresponding cross section in each target foil was calculated from the primary experimental data (number of target atoms per unit surface N_t, number of bombarding particles per unit time N_b, net peak area of the photo-peak T_γ, detector efficiency ε_d, gamma ray intensity ε_γ, measurement dead time ε_t, decay constant λ, bombarding time t_b, cooling time t_c and acquisition time t_m) according to the well known activation formula for charged particle activation Eq. 1.

$$\sigma = \frac{T_\gamma \lambda}{\varepsilon_d \varepsilon_\gamma \varepsilon_t N_t N_b \left(1 - e^{-\lambda t_b}\right) e^{-\lambda t_c} \left(1 - e^{-\lambda t_m}\right)} \qquad (1)$$

The formula includes corrections for decay of the investigated radionuclides during irradiation, cooling and measurment time. Nuclear decay data of the investigated radionuclides and reaction Q-values were taken from the corresponding on-line NuDat2.6 database [24] and QCalc calculation tool [25] respectively and are summarized in Table 1.

Table 1. Decay data of the investigated radionuclides and list of contributing reactions. For emission of complex particles the Q-values have to be corrected by the respective binding energies of the outgoing particles: deuteron: 2.2 MeV; triton: 8.48 MeV; ^{3}He: 7.72 MeV; α: 28.30 MeV.

	half life	E_γ keV	I_γ %	Contributing Reactions	Threshold Energy MeV	Q-value MeV
^{72}Se	8.4 d	45.89	57.2	^{70}Ge(α,2n)	17.35	-16.41
				^{72}Ge(α,4n)	36.50	-34.58
				^{73}Ge(α,5n)	43.63	-41.36
^{73m}Se	39.8 min	67.07	2.6	^{70}Ge(α,n)	8.44	-7.98
	IT: 72.6%	84.0	2.03	^{72}Ge(α,3n)	27.60	-26.15
	ε: 27.4 %	253.7	2.36	^{73}Ge(α,4n)	34.74	-32.93
				^{74}Ge(α,5n)	45.46	-43.13
^{73g}Se	7.15 h	67.07	70	^{70}Ge(α,n)	8.44	-7.98
		361.2	97	^{72}Ge(α,3n)	27.60	-26.15
				^{73}Ge(α,4n)	34.74	-32.93
				^{74}Ge(α,5n)	45.46	-43.13
^{75}Se	119.78 d	121.115	17.2	^{72}Ge(α,n)	6.40	-6.06
		136	58.5	^{73}Ge(α,2n)	13.55	-12.85
		264.66	58.9	^{74}Ge(α,3n)	24.29	-23.04
		279.54	25.02	^{76}Ge(α,5n)	41.03	-38.98
		400.66	11.41			
^{71}As	65.3 h	175.0	82.4	^{70}Ge(α,p2n)	25.03	-23.68
		326.8	3.05	^{72}Ge(α,p4n)	44.17	-41.84
		1095.49	4.1	^{73}Ge(α,p5n)	51.29	-48.63
^{72}As	26.0 h	834.0	80.0	^{70}Ge(α,pn)	16.14	-15.27
		630.0	7.92	^{72}Ge(α,p3n)	35.29	-33.43
		894.3	0.79	^{73}Ge(α,p4n)	42.42	-40.22
				^{74}Ge(α,3nt)	44.20	-41.93
^{74}As	17.77 d	595.8	59	^{72}Ge(α,pn)	15.48	-14.66
		634.8	15.4	^{73}Ge(α,p2n)	22.62	-21.44
				^{74}Ge(α,p3n)	33.35	-31.64
				^{76}Ge(α,p5n)	50.08	-47.57
^{76}As	26.24 h	559.1	45.0	^{73}Ge(α,p)	4.08	-3.87
		657.1	6.2	^{74}Ge(α,pn)	14.83	-14.07
		1216.1	3.4	^{76}Ge(α,p3n)	31.58	-30.00
^{78}As	90.7 min	613.8	54	^{76}Ge(α,pn)	14.03	-13.33
		694.9	16.7			
		1308.7	13			
^{69}Ge	39.05 h	872.0	11.9	^{70}Ge(α,αn)	12.19	-11.53
		1106.8	36	^{72}Ge(α,α3n)	31.35	-29.70
				^{73}Ge(α,α4n)	38.48	-36.48
				^{74}Ge(α,α5n)	49.21	-46.68
^{72}Ga	14.1 h	629.967	26.13	^{72}Ge(α,3pn)	33.26	-31.51
		834.13	95.45	^{73}Ge(α,αp)	10.55	-10.00
		894.327	10.136	^{74}Ge(α,αpn)	21.29	-20.19
				^{76}Ge(α,αp3n)	38.03	-36.13

2.5. Uncertainties

The uncertainty of the deduced cross section data was estimated as the square root of the quadratic summation of the relative, independently contributing error components. The uncertainty assigned to the deduced cross section data includes the following components: number of incident charged particles per unit time (4%), number of target nuclei (5%), decay data (3%), energy dependent detector efficiency (4-9 %), and statistical uncertainty on total energy peak area (1-8%) (in cases of overlapping of complex peaks (15-25%)). The overall uncertainty corresponds to 9-14% (17-28% for radionuclides with interfering gamma-lines). The uncertainty of the time parameters (irradiation, cooling and measuring time) was not included. For long half-life radionuclides contribution of uncertainties of time parameters can be neglected. The initial uncertainty of the bombarding energy was ±0.2 MeV which increased gradually as the beam penetrated into the target due to straggling effects and target thickness uncertainty. The uncertainty of the energy scale originates mainly from the cumulative effects of the uncertainty of the energy loss calculation. The uncertainty of the layer thicknesses influences the layer-by-layer stopping calculation for the stack. The overall energy uncertainty increases throughout the stack from ±0.2 MeV (first Ge layer) up to ±1.2 MeV (last Ge layer) for the RIKEN experiment and from ±0.3 MeV up to ±0.5 MeV for the short stacks of the Atomki experiments.

3. Model calculations

In this work no dedicated model calculation was performed. Instead, results of a-priori model calculations were compared to the deduced experimental cross section data. The tabulated data are results of model calculations based on the standard input parameters and the latest version of the TALYS code system. The estimated results were taken from the tabulated TENDL data library available on-line [26]. For each investigated process, the involved individual reaction cross section data were retrieved from the database, then they were normalized to the natural isotopic abundance of the Ge target and summed up to be able to compare with the measured experimental production cross section for a given reaction product. The comparison showed disagreement among the measured and calculated values in most cases. Detailed analysis of the disagreement trends between the measured and calculated cross sections may explain the differences among them and can contribute to the development of the used theoretical models as well as revision of the computer code.

4. Results

On the five stable isotopes of Ge several reactions can take place and result in production of series of different radionuclides at the used 50 MeV bombarding energy. It is obvious that the experimental conditions cannot be optimized for all the reaction products in one irradiation. Reaction products with half-lives longer than about 1 h were possible to identify and investigate at the used irradiation parameters and measuring conditions. The excitation functions deduced from the measurements for the investigated processes are presented in Figs. 2-10 in comparison with the available data from previous experiments. The retrieved results of the TALYS calculation from TENDL library also included in the corresponding figure. The numerical cross sections data are presented in Tables 2 and 3.

4.1. Production of selenium radioisotopes

Selenium isotopes can be produced on natural Ge targets in (α,xn) processes. The initial E_α = 51.25 MeV bombarding particle energy makes possible production of selenium isotopes with mass numbers from 70 to 80. Due to the experimental constrains we could only deduce cross section data for the reaction products of ^{72,73,75}Se.

4.1.1. Production of ^{72}Se

Selenium-72 has a half-life of 8.4 d. Its decay is followed by emission of only low energy gamma photons at E_γ = 45.89 keV. This energy was out of the measuring range of the used detector set-up, therefore the activity of the produced ^{72}Se was determined using the gamma-lines of its shorter-lived ^{72}As daughter nuclide in secular equilibrium. The measurement was done after a long cooling time when the directly-produced ^{72}As was considered to be decayed away completely.

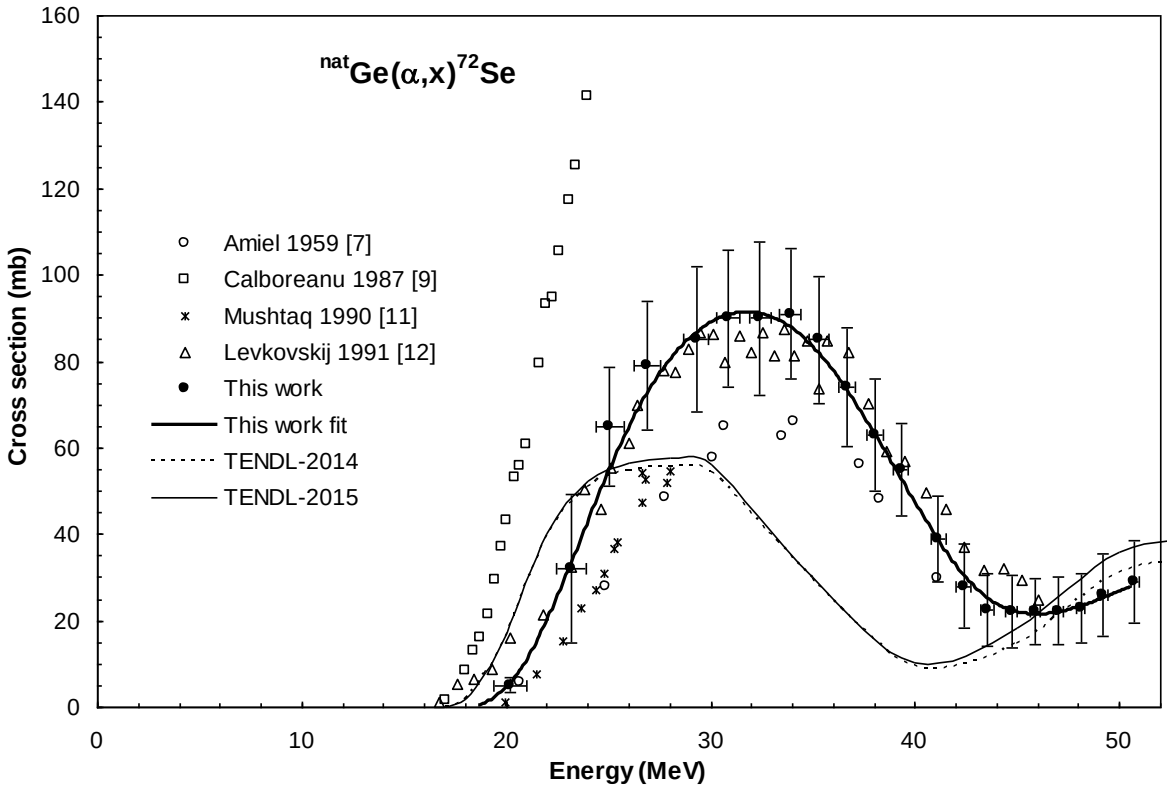

Figure 2. Experimental cross section data for the ^{nat}Ge(α,x)^{72}Se reaction in comparison with the earlier measured data and the results of theoretical calculations. The thick solid line is a spline fit over the experimental points measured in this work.

For production of ^{72}Se isotope on natural Ge target, the main contributing reaction is the ^{70}Ge(α,2n)^{72}Se. It is the only reaction up to E_α = 36.5 MeV, to the threshold energy of the ^{72}Ge(α,4n)^{72}Se reaction. The ^{72}Se decays to ^{72}As. Since ^{72}As and ^{72}Ga isotopes are produced simultaneously in different processes and probabilities their contribution should be eliminated from the measured photo peak. Applying long cooling time the contribution of these two decaying radionuclides can be neglected and the activity of ^{72}Se in secular equilibrium with

^{72}As can be measured. The cross section data measured in this work are shown in Fig.2 and the numerical values are collected in Table 2. There are four earlier measured datasets. Out of them the Calboreanu's data [9] clearly overestimates the cross section. It may contain contribution from decay of ^{72}As and ^{72}Ga isotopes if it was measured via the decay of ^{72}As. A clear explanation of their high values was not found. The data of Amiel [7] and Mushtaq [11] are somewhat lower than our result. The normalized data of Levkovskij [12], which were measured on enriched Ge target isotopes, have good agreement with our cross sections regarding both the amplitude and the shape of the excitation function. The TALYS theoretical model calculation provides an excitation function with lower amplitude and an energy scale shifted toward lower energy. Results were taken from the TENDL data library.

4.1.2. Production of ^{73}Se

The radionuclide ^{73}Se has two isomeric states, the E = 25.7 keV excited state with $T_{½}$ = 39.8 min and the ground state with $T_{½}$ = 7.15 h half-life. The higher energy excited state decays to the ground state by IT decay mode with 72.6%, while the remaining 27.3% decays directly to ^{73}As. The data analysis was based on the spectra measured after more than 10 h cooling time. This long cooling time assured decay of the excited state below the detection limit. The intense gamma-line, E_γ = 361.2 keV, was used to assess the activity of the ^{73g}Se radionuclide which contains contribution of 72.6% from ^{73m}Se. The numerical values of the cross sections deduced in this work are collected in Table 2 and are shown in Fig. 3 together with the literature data and results of theoretical calculations. Below E_α = 27.6 MeV bombarding particle energy, the only contribution to the total activity is the ^{70}Ge(α,n)^{73}Se reaction. The higher energy hump of the excitation function may contain contributions from the ^{72}Ge(α,3n), ^{73}Ge(α,4n) and ^{74}Ge(α,5n) reactions. The earlier measured data form two groups. The data of Guillaume [8], Calboreanu [9] and the normalized ones of Levkovskij [12] form a lower amplitude group, while the data of Qaim [10] and Mushtaq [11] form higher amplitude one. The difference between these two groups is roughly a factor of two at maximum. While data of Calboreanu [9] for ^{72}Se represent the highest value in this case their data are in the lower amplitude group. Data of Mushtaq [11] belong to the higher amplitude group for the ^{nat}Ge(α,x)^{73}Se case, but their data represents one of the lowest results in the case of ^{72}Se. Overall the earlier experimental data are scattered both in amplitude and in energy scale. The theoretical estimation for the low energy bump around Eα = 20 MeV for the ^{70}Ge(α,n)73Se reaction is even lower than the lower amplitude experimental data group, while the theoretical estimation for the high energy bump around Eα = 40 MeV is considerably higher than the experimental data.

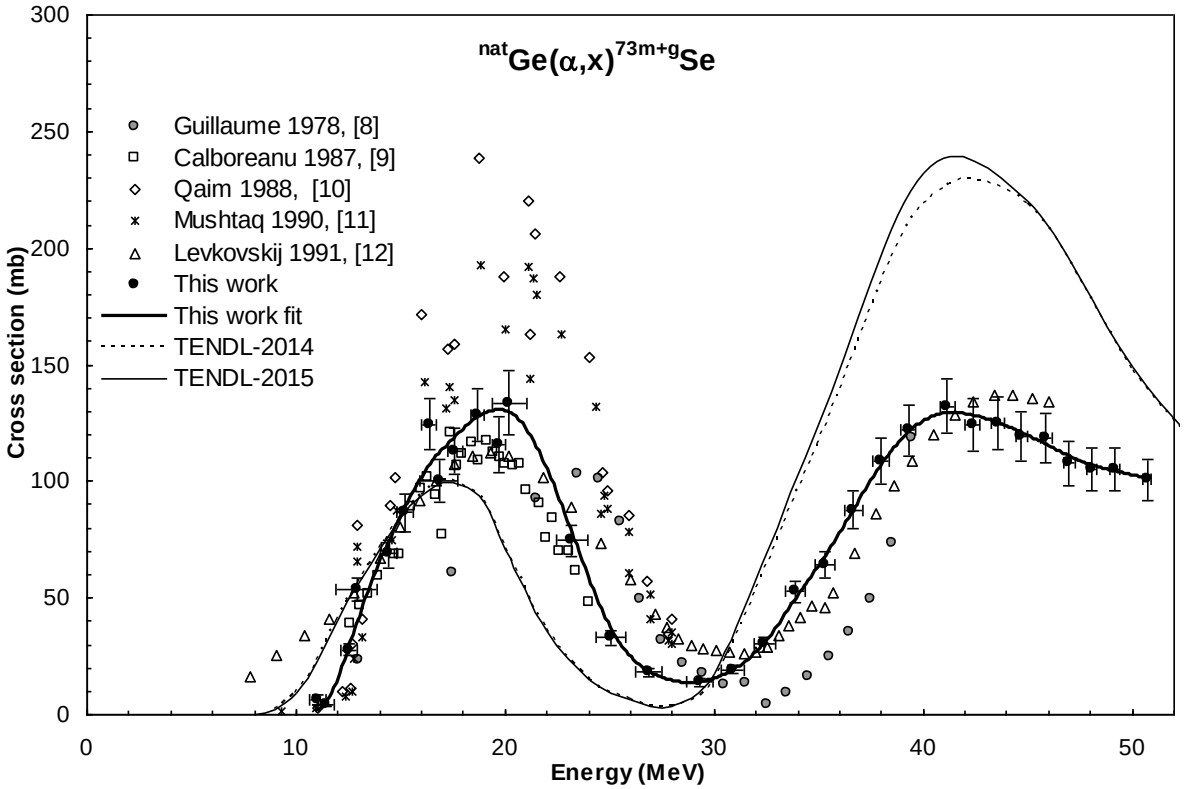

Figure 3. Experimental cross section data for the $^{nat}Ge(\alpha,x)^{73m+g}Se$ reaction in comparison with the available literature data and the result of the theoretical calculations. The thick solid line is a spline fit over the experimental points measured in this work.

4.1.3. Production of ^{75}Se

The long-lived ^{75}Se ($T_{½}$ = 119.78 d) was assessed from the spectra measured after a long cooling time. The activity determination was straightforward, since the decay of ^{75}Se is followed by several strong interference free gamma-lines. ^{75}Se can be produced on four stable isotopes of germanium by the $^{72}Ge(\alpha,n)$, $^{73}Ge(\alpha,2n)$, $^{74}Ge(\alpha,3n)$ and $^{76}Ge(\alpha,5n)$ reactions with different yields. Our experimental data are presented in Fig. 4 together with the calculated spline fit, the earlier reported experimental data, and the result of the TALYS calculation. The numerical values of our newly measured, elemental cross section data are listed in Table 2. The excitation function has a double bump around E_α = 18 MeV and E_α = 38 MeV respectively. There are two earlier measured data sets. Data of Levkovskij [12] agree with our data within experimental uncertainties above 20 MeV at lower energies systematic shift of the energy scale can be observed. The data of Mushtaq [11] are scattered very much and are higher around the first local maximum of the excitation function. The TALYS calculation could not reproduce properly the experimental data. The amplitude of the calculated excitation function is too small for the first local maximum of the curve and the high energy maximum is completely missing.

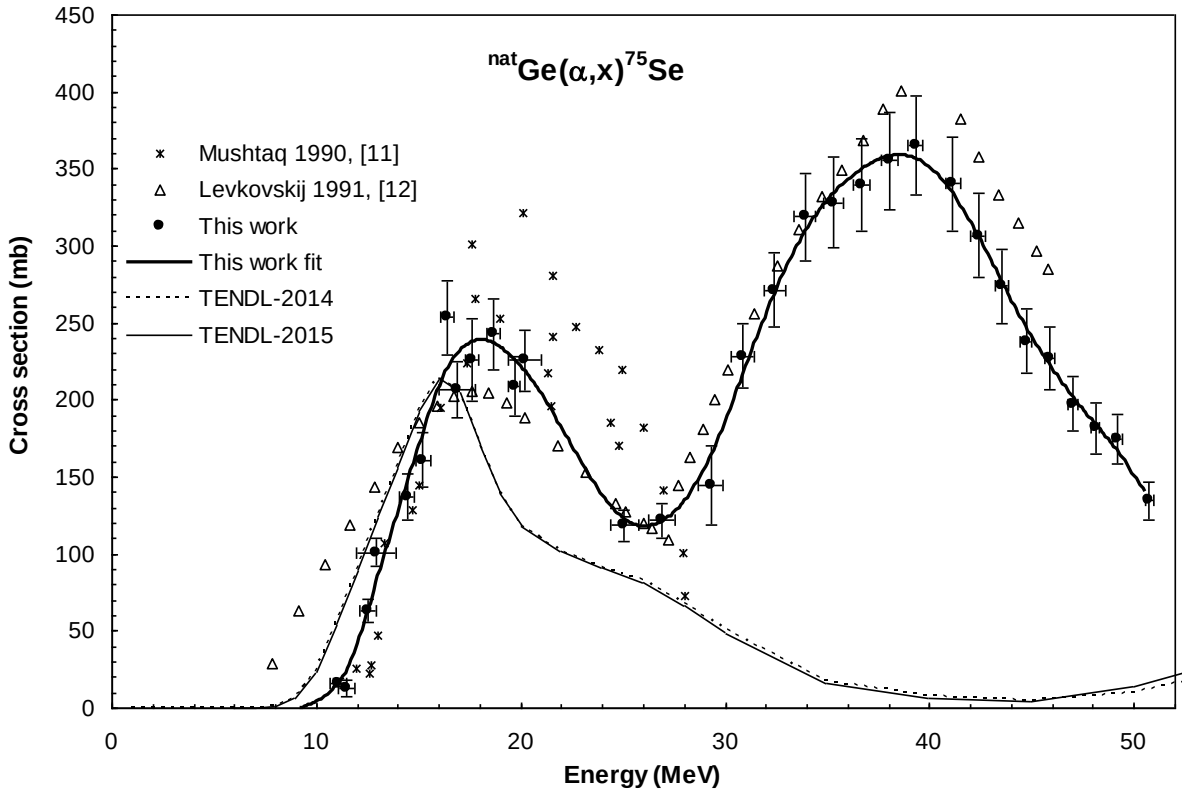

Figure 4 Experimental cross section data for the $^{nat}Ge(\alpha,x)^{75}Se$ reaction in comparison with the earlier measured data and the result of the theoretical calculations. The thick solid line is a spline fit over the experimental points measured in this work.

Table 2. Experimental activation cross sections of the $^{nat}Ge(\alpha,x)^{72,73,75}Se$ and $^{nat}Ge(\alpha,x)^{69}Ge$ processes

Energy	Cross section (mb)			
MeV	$^{nat}Ge(a,x)^{72}Se$	$^{nat}Ge(a,x)^{73m+g}Se$	$^{nat}Ge(a,x)^{75}Se$	$^{nat}Ge(a,x)^{69}Ge$
50.73 ± 0.20	29.1 ± 9.4	100.7 ± 9.0	134.6 ± 12.0	21.4 ± 2.0
49.17 ± 0.22	26.1 ± 9.5	105.1 ± 9.4	174.8 ± 15.8	17.4 ± 1.8
48.09 ± 0.24	23.0 ± 8.1	105.2 ± 9.4	181.9 ± 16.5	16.3 ± 1.5
46.99 ± 0.25	22.3 ± 7.7	107.8 ± 9.6	197.5 ± 17.6	15.5 ± 1.4
45.86 ± 0.27	22.1 ± 7.6	118.4 ± 10.6	227.2 ± 20.3	16.3 ± 1.5
44.71 ± 0.29	22.1 ± 8.4	119.2 ± 10.6	238.3 ± 21.3	16.2 ± 1.5
43.54 ± 0.31	22.5 ± 8.4	124.9 ± 11.1	273.9 ± 24.4	17.6 ± 1.7
42.35 ± 0.33	28.0 ± 9.7	124.1 ± 11.1	306.6 ± 27.4	19.4 ± 1.8
41.13 ± 0.35	39.0 ± 9.8	132.3 ± 11.8	340.5 ± 30.3	23.7 ± 2.2
39.29 ± 0.38	55.1 ± 10.7	121.9 ± 10.9	365.3 ± 32.5	26.6 ± 2.4
38.00 ± 0.40	63.2 ± 13.1	108.7 ± 9.8	355.5 ± 31.7	26.7 ± 2.5
36.67 ± 0.43	74.1 ± 13.7	87.8 ± 7.9	339.7 ± 30.1	25.3 ± 2.4
35.29 ± 0.47	85.1 ± 14.8	64.2 ± 5.9	328.3 ± 29.3	25.5 ± 2.4
33.87 ± 0.50	91.0 ± 15.1	52.6 ± 4.9	318.9 ± 28.5	27.1 ± 2.5
32.40 ± 0.53	90.0 ± 17.6	30.0 ± 3.1	271.5 ± 24.4	24.8 ± 2.3
30.88 ± 0.57	90.1 ± 15.8	19.3 ± 1.9	228.6 ± 21.0	21.6 ± 2.0
29.29 ± 0.61	85.1 ± 16.8	13.9 ± 1.5	144.4 ± 25.6	18.6 ± 1.9
26.85 ± 0.65	79.1 ± 14.8	18.0 ± 1.8	121.8 ± 11.0	13.1 ± 1.4
25.07 ± 0.69	65.2 ± 13.8	33.0 ± 3.0	118.5 ± 10.5	8.3 ± 0.9
23.18 ± 0.75	32.5 ± 17.3	74.5 ± 6.7		1.2 ± 0.2
20.21 ± 0.82	5.0 ± 1.7	133.8 ± 13.8	225.6 ± 20.0	0.38 ± 0.06
19.68 ± 0.31	3.0 ± 0.3	115.7 ± 12.1	209.0 ± 19.4	
18.66 ± 0.32	0.3 ± 0.1	128.4 ± 11.4	243.1 ± 23.1	
17.60 ± 0.33		113.1 ± 10.0	226.0 ± 26.9	
16.85 ± 0.90		100.2 ± 8.9	206.6 ± 18.3	0.16 ± 0.01
16.38 ± 0.35		124.6 ± 11.1	253.6 ± 24.1	
15.21 ± 0.36		86.6 ± 8.0	161.1 ± 17.6	
14.43 ± 0.37		68.9 ± 6.1	136.9 ± 14.9	
12.91 ± 0.98		53.6 ± 4.7	100.9 ± 9.1	0.03 ± 0.01
12.50 ± 0.39		27.7 ± 2.5	63.6 ± 7.4	
11.43 ± 0.40		4.2 ± 0.4	12.8 ± 5.6	
11.04 ± 0.40		6.3 ± 2.2	16.5 ± 2.9	

4.2. Production of arsenic radioisotopes

Arsenic isotopes from ^{68}As to ^{79}As can be produced through (α,pxn) processes on natural germanium targets in alpha particle bombardment at E_α = 52 MeV particle energy. Beside the emission of proton and neutrons, reactions with deuteron and/or triton complex particles in the exit channel are also possible. These reactions have lower threshold energies but their probability is smaller, too. The As isotopes except ^{74}As and ^{76}As can also be produced in the decay of the isobaric parent Se and/or Ge radioisotopes. Since the half-lives of $^{68,69,70}As$ and ^{79}As are too short compared to the applied cooling time, these four radionuclides could not be assessed properly in this work. Also, ^{73}As could not be detected due to its low energy gamma-photons which were out of the detection range. For assessing ^{77}As, due to its very weak gamma lines, the collected counts under the peaks were not enough to provide useful information on the cross section. The processes resulting in formation of $^{71,72,74,76,78}As$ were hence studied by using activation technique in this work.

4.2.1. Production of ^{71}As

The radionuclide ^{71}As has a half-life of 65.3 h which makes the determination of its activity convenient. ^{71}As is produced in the $^{70}Ge(\alpha,p2n)$, $^{72}Ge(\alpha,p4n)$ and $^{73}Ge(\alpha,p5n)$ reactions (including *d* and *t* particles in the exit channel). Contribution from reactions on ^{72}Ge and ^{73}Ge target isotopes are of importance only above E_α = 35 MeV and E_α = 42 MeV respectively.

The activity of ^{71}As was assessed from the spectra acquired in the second series. Decay of ^{71}As is followed by emission of several weak gamma-lines with one exception. The E_γ = 174.9 keV gamma-line (I_γ = 82.4 %) was used to determine the activity of the ^{71}As isotope. The deduced cross sections are considered to be cumulative elemental cross sections since production through decay of ^{71}Se is also possible. The numerical values are collected in Table 3. The new experimental points and their spline fit are presented in Fig. 5 together with the earlier measured experimental cross section data and the result of the TALYS calculation taken from the TENDL data library.

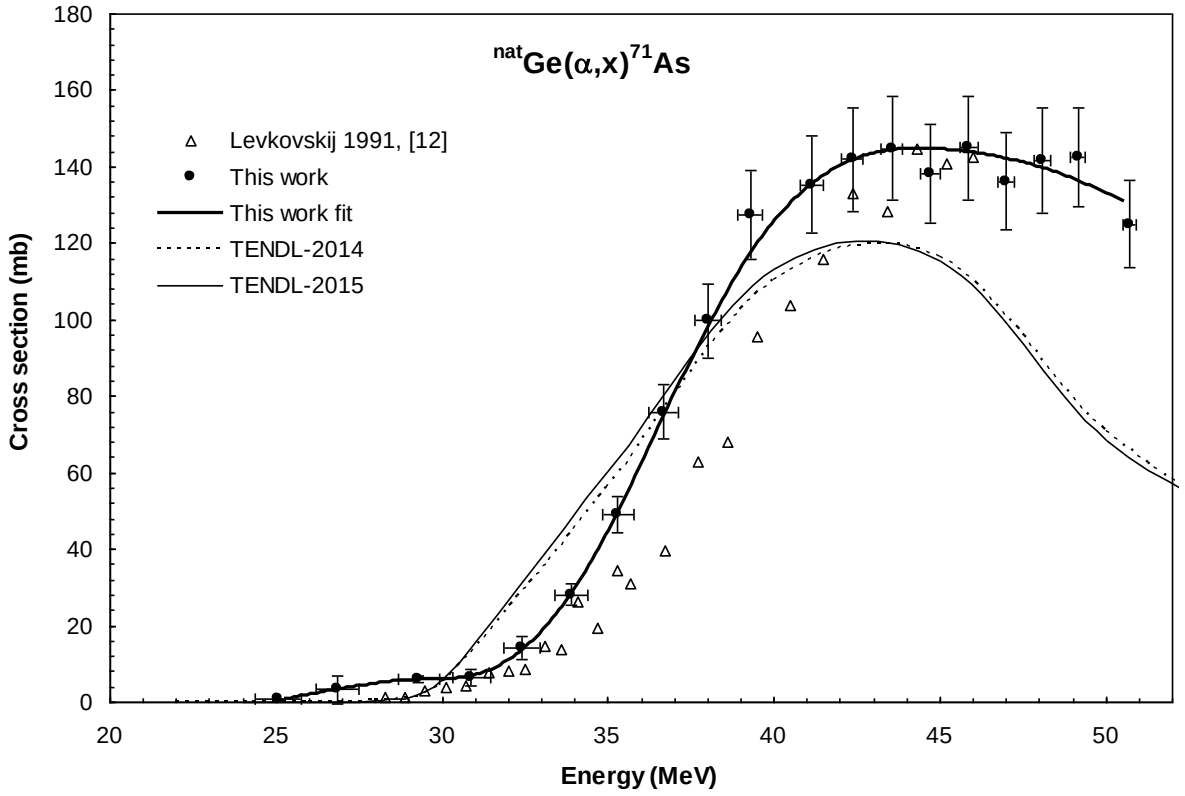

Figure 5. Experimental cross section data for the ^{nat}Ge(α,x)^{71}As reaction in comparison with the earlier measured data and the result of the theoretical calculations. The thick solid line is a spline fit over the experimental points measured in this work.

There is only one set of earlier measured experimental data, published by Levkovskij [12], on enriched ^{70}Ge target. The reproduced data points were normalized to natural isotopic abundance. Levkovskij's data are agreeing with the same extent with our newly measured cross sections as in all the above cases, meaning similar amplitude and small shift of the energy to higher values. The TALYS code also indicates much steeper decrease of the excitation functions for E_α > 46 MeV than observed in the experiment.

4.2.2. Production of ^{72}As

The ^{72}As ($T_{½}$ = 26 h) can be produced directly, and by decay of ^{72}Se parent radionuclide indirectly. Several reactions can contribute to its production considering both direct and indirect production routes. The elemental cross section of the process as sum of the direct contributing reactions on four stable isotopes of germanium, the ^{70}Ge(α,pn), ^{72}Ge(α,p3n),

^{73}Ge(α,p4n), and ^{74}Ge(α,3nt) as well as the reactions with *d* and *t* particles in the exit channel, can be determined after decay of the interfering ^{72}Ga ($T_{½}$ = 14 h) isobar radionuclide. Both isobars the ^{72}As and ^{72}Ga decay to ^{72}Ge therefore have common gamma-lines. In the assessment of ^{72}As the three most intense gamma-lines were used: E_γ = 630 keV, E_γ = 834 keV and E_γ = 894 keV. Contribution from decay of ^{72}Se was subtracted and contribution from ^{72}Ga was neglected due to the applied cooling time and the low production cross section of ^{72}Ga. Thus, the presented data are elemental and direct production cross section for ^{72}As on natural Ge target. The newly measured experimental data and its spline fit are shown in Fig. 6, together with the only earlier measured data by Levkovskij [12] and the result of the theoretical calculations. The numerical data are collected in Table 3. Our data are about 15% lower than those of Levkovskij [12] at the maximum of the excitation function and its peak is narrower. The theoretical estimations somewhat overestimate the experimental data around the low energy local maximum and are considerably higher at higher energies.

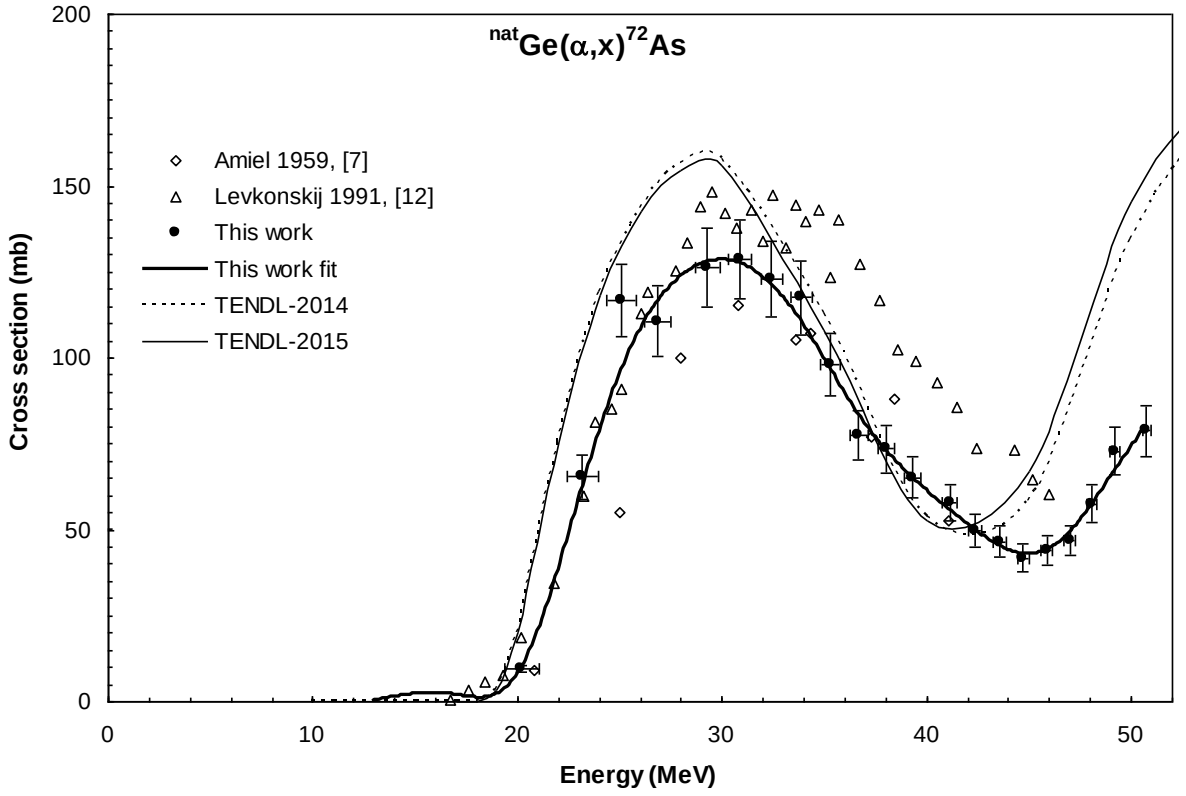

Figure 6 Experimental cross section data for the ^{nat}Ge(α,x)^{72}As reaction in comparison with the earlier measured data and the result of the theoretical calculations. The thick solid line is a spline fit over the experimental points measured in this work.

4.2.3. Production of ^{74}As

The radionuclide ^{74}As can be produced in the ^{72}Ge(α,pn), ^{73}Ge(α,p2n), ^{74}Ge(α,p3n) and ^{76}Ge(α,p5n) reactions, and also in the reactions with lower probability on the same Ge target isotopes with *d* and *t* particle emissions in the exit channels. Interference from decay of ^{74}Ga can be neglected due to its short half-life ($T_{½}$ = 8.1 min) of that isotope. The radionuclide ^{74}As can be assessed by its intense E_γ = 595.83 keV gamma-line. This gamma-line can be still considered as an independent one although there are interfering gamma-lines from decay of

^{70}As and ^{71}As, but their effect can be neglected due to their shorter half-lives. The spectra taken in the third measurement series were used for assessing this radioisotope.

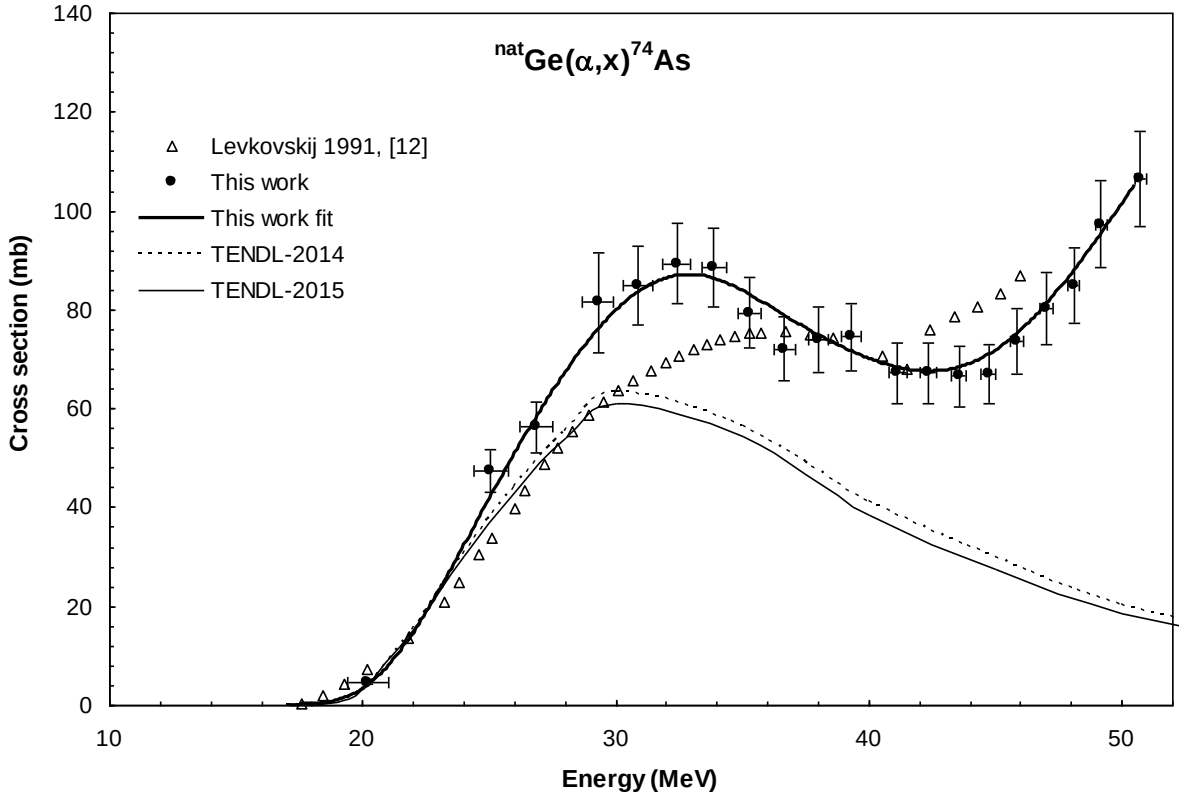

Figure 7. Experimental cross section data for the ^{nat}Ge(α,x)^{74}As reaction in comparison with the earlier measured data and the result of the theoretical calculations. The thick solid line is a spline fit over the experimental points measured in this work.

The presented cross sections are considered as independent elemental cross sections. The experimental results are presented in Fig. 7 and also listed in Table 3. Only one dataset was found in the literature measured by Levkovskij [12]. His excitation function has about the same amplitude but a slightly different shape. The prediction of the TALYS calculations for this process is not good: the result of TALYS calculation is in acceptable agreement with the experimental data up to about E_α = 30 MeV, but the high energy rising part of the experimental data is not represented properly.

4.2.4. Production of ^{76}As

Reactions ^{73}Ge(α,p), ^{74}Ge(α,pn) and ^{76}Ge(α,p3n) on three Ge target isotopes contribute to the production of 76As (including also emission of d and t particles in the exit channel). This radioisotope was assessed by using the only strong E_γ = 559.1 keV gamma-line which is in interference with gamma-lines of ^{69}As, ^{67}Ge, ^{77}Ge and ^{66}Ga, within the resolution of the detector. Due to the short half-life and the corresponding low gamma intensity of the isotope ^{69}As its contribution was neglected. The possible interference with ^{67}Ge and ^{66}Ga can be neglected due to their very low intensity gamma-lines. The possible contribution from decay of ^{77}Ge was also neglected, since its more intense and independent gamma-lines were not observed. The presented cross sections are considered as independent elemental cross sections.

The new experimental results are presented in Fig. 8 together with the spline fit, the earlier measured data, and the result of the TALYS calculation taken from the TENDL data library. The numerical data are presented in Table 3.

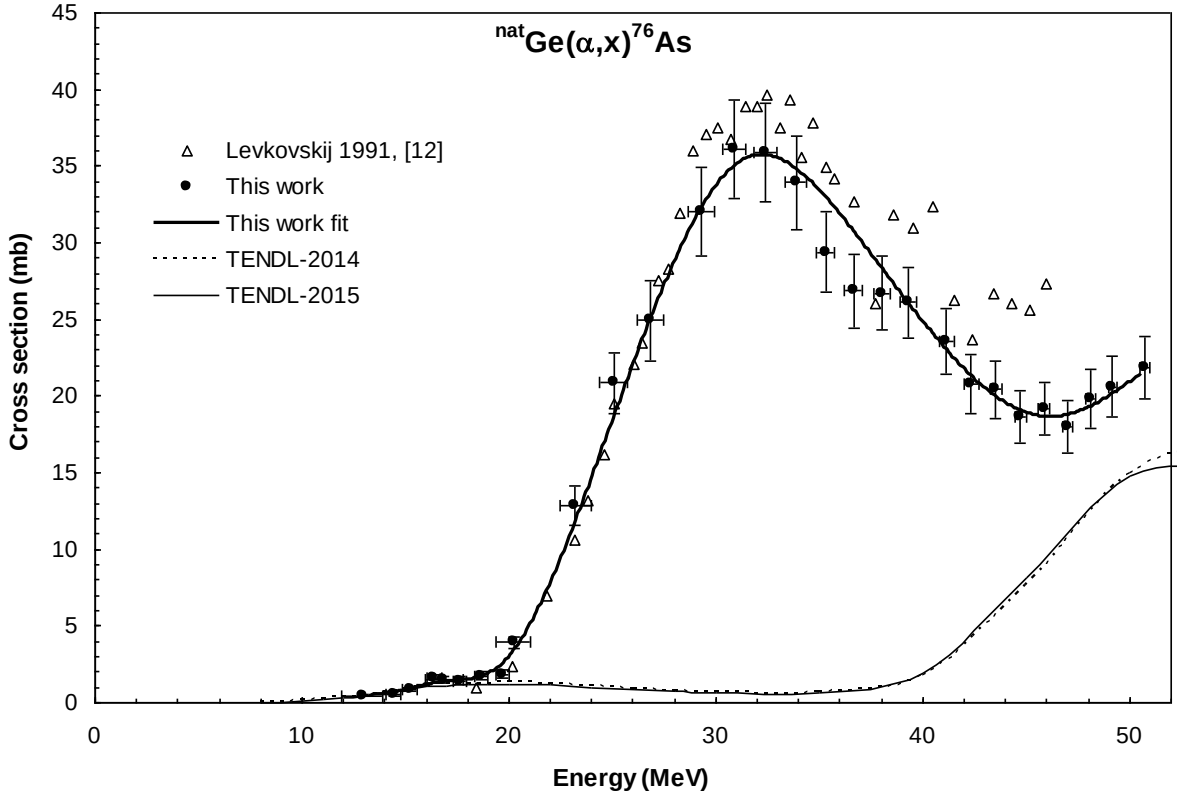

Figure 8. Experimental cross section data for the $^{nat}Ge(\alpha,x)^{76}As$ reaction in comparison with the earlier measured data and the result of the theoretical calculations. The thick solid line is a spline fit over the experimental points measured in this work.

Again only one experimental data set was found in the literature measured by Levkovskij [12] on enriched target isotopes. His data were normalized to natural isotopic abundances and were combined to be able to compare them with our elemental cross sections. For this process, the reported data of Levkovskij are somewhat higher than our results but have the similar shape. The theoretical calculation underestimates the experimental data very much and the shape of the calculated excitation function is completely different from the experimental one.

4.2.5. Production of ^{78}As

The radionuclide ^{78}As can be produced only on ^{76}Ge in the $^{76}Ge(\alpha,pn)$ reaction. With lower probability, also emission of deuteron is possible in the exit channel. The $T_{½}$ = 90.7 min half-life and the E_γ = 613.8 keV intense gamma-line make easy to determine its activity. In principle, there are potential interfering gamma-lines from ^{71}As and ^{77}Ge, but their contributions are negligible due to their low emission probability. The presented data are considered as independent elemental cross sections. The new experimental results are presented in Fig. 9 together with the spline fit, the earlier measured data, and the result of TALYS calculation. The numerical data can be found in Table 3. For this reaction again only

one earlier experimental data set is available, measured by Levkovskij [12]. His normalized data are also shown in Fig. 9. The reported cross section data of Levkovskij are in agreement with our result. They form a similar shape and have similar amplitude. The theoretical calculation underestimates the experimental data especially above E_α = 30 MeV.

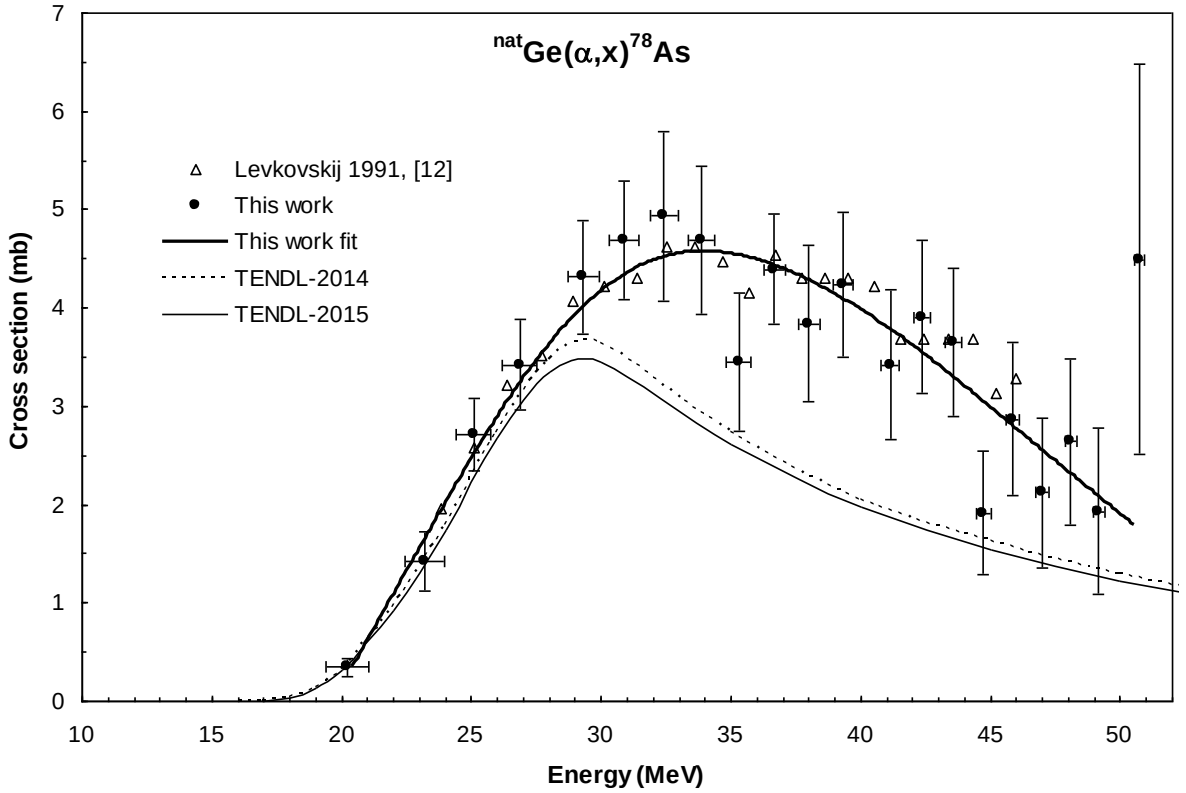

Figure 9 Experimental cross section data for the $^{nat}Ge(\alpha,x)^{78}As$ reaction in comparison with the earlier measured data and the result of the theoretical calculations. The thick solid line is a spline fit over the experimental points measured in this work.

4.3. Production of Ge radioisotopes

Production of Ge isotopes is possible in (α,αxn) processes on natural germanium targets by ^{4}He bombardment, including emission of combination of other particles in the exit channel (proton, deuterons, tritons and ^{3}He). Ge isotopes can also be produced by decay of the isobaric parent As and/or Ga radioisotopes. The applied E_α = 51.25 MeV beam energy allows production of Ge isotopes with mass numbers between 66 and 78. Considering the decay parameters of the possible produced Ge isotopes and the used experimental circumstances, we were able to assess confidently only the ^{69}Ge.

4.3.1. Production of ^{69}Ge

Although the threshold energy of the $^{70}Ge(\alpha,\alpha n)$ reaction for direct production of ^{69}Ge is E_{th} = 12.2 MeV, the apparent threshold of the reaction is around E_α = 20 MeV. The indirect production of ^{69}Ge by decay of ^{69}As may start around E_α = 40 MeV bombarding particle

energy. The newly measured cross sections are presented in Fig. 10 and in Table 2. The measured excitation function has a relative complex shape. Emission of several gamma-lines follow the decay of ^{69}Ge radionuclide among them there are two relatively strong ones the E_γ = 872 keV and the E_γ = 1106.8 keV. These two gamma-lines can be considered interference free. For the assessment of the activity of ^{69}Ge both gamma-lines were used and the simple mathematical average of the deduced cross sections was calculated. Only one earlier experimental data set was found in the literature published by Levkovskij [12]. The excitation function starts above E_α = 12 MeV and stay very low up to about E_α = 20 MeV than rises rapidly to about E_α = 35 MeV reaching a local maximum of about 27 mb. Above E_α = 46 MeV where the excitation function has a local minimum the cross section raises again. The TALYS calculation taken from the TENDL data library predicts the shape of the excitation function relatively well but above E_α = 48 MeV the theoretical estimation become too high when compared to the experimental data.

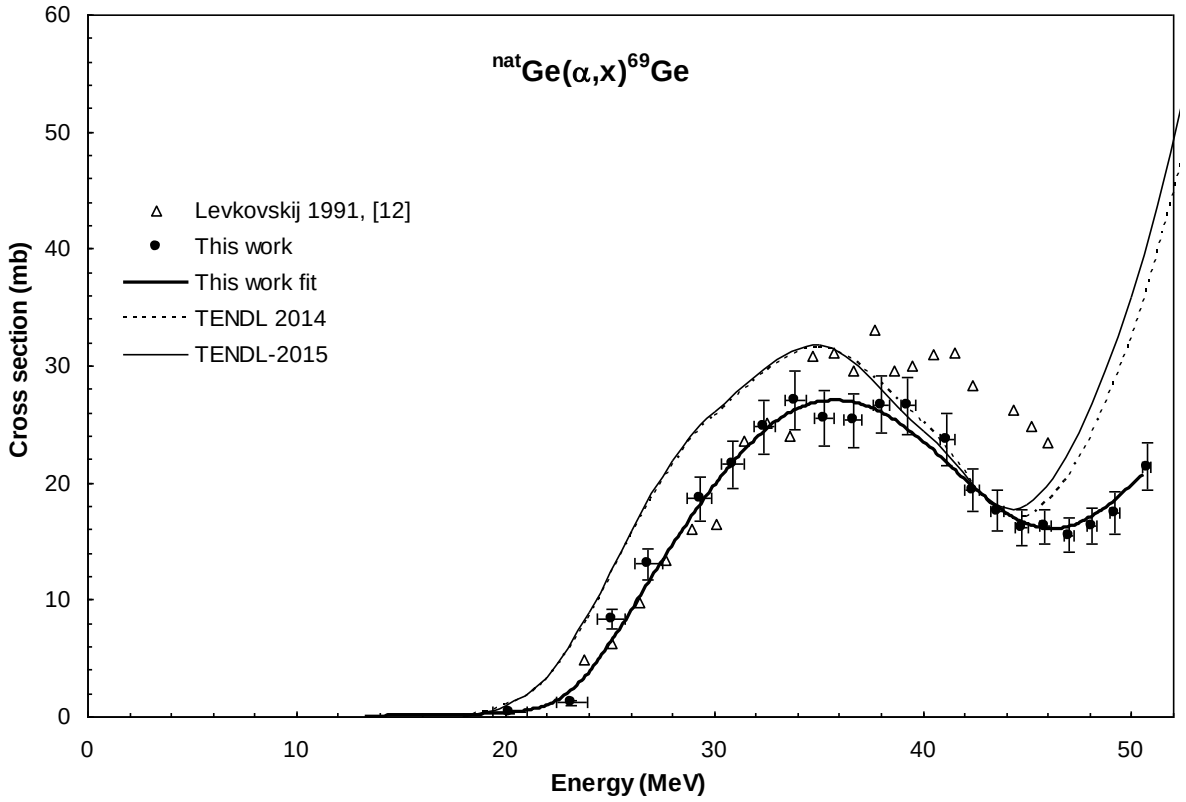

Figure 10. Experimental cross section data for the ^{nat}Ge(α,x)^{69}Ge reaction in comparison with the earlier measured data and the result of the theoretical calculations. The thick solid line is a spline fit over the experimental points measured in this work.

Table 3. Experimental activation cross sections of the $^{nat}Ge(\alpha,x)^{71,72,74,76,78}As$ processes

Energy	Cross section (mb)				
MeV	$^{nat}Ge(\alpha,x)^{71}As$	$^{nat}Ge(\alpha,x)^{72}As$	$^{nat}Ge(\alpha,x)^{74}As$	$^{nat}Ge(\alpha,x)^{76}As$	$^{nat}Ge(\alpha,x)^{78}As$
50.73 ± 0.20	125.1 ± 11.4	78.8 ± 7.3	106.5 ± 9.5	21.9 ± 2.1	4.5 ± 2.0
49.17 ± 0.22	142.6 ± 13.0	72.9 ± 6.9	97.3 ± 8.8	20.6 ± 2.0	1.9 ± 0.8
48.09 ± 0.24	141.8 ± 13.8	57.6 ± 5.4	85.0 ± 7.7	19.8 ± 1.9	2.6 ± 0.8
46.99 ± 0.25	136.2 ± 12.7	47.0 ± 4.5	80.3 ± 7.2	18.0 ± 1.7	2.1 ± 0.8
45.86 ± 0.27	144.9 ± 13.6	43.9 ± 4.2	73.7 ± 6.6	19.2 ± 1.7	2.9 ± 0.8
44.71 ± 0.29	138.2 ± 12.9	41.7 ± 4.0	67.0 ± 6.1	18.7 ± 1.7	1.9 ± 0.6
43.54 ± 0.31	144.8 ± 13.6	46.6 ± 4.4	66.6 ± 6.0	20.4 ± 1.9	3.6 ± 0.8
42.35 ± 0.33	141.9 ± 13.5	49.8 ± 4.7	67.2 ± 6.1	20.8 ± 1.9	3.9 ± 0.8
41.13 ± 0.35	135.4 ± 12.8	57.9 ± 5.4	67.2 ± 6.1	23.5 ± 2.1	3.4 ± 0.8
39.29 ± 0.38	127.5 ± 11.7	65.2 ± 6.0	74.5 ± 6.7	26.1 ± 2.3	4.2 ± 0.7
38.00 ± 0.40	99.7 ± 9.5	73.5 ± 6.8	74.1 ± 6.7	26.7 ± 2.4	3.8 ± 0.8
36.67 ± 0.43	76.0 ± 7.1	77.7 ± 7.2	72.1 ± 6.4	26.9 ± 2.4	4.4 ± 0.6
35.29 ± 0.47	49.3 ± 4.8	98.1 ± 8.9	79.4 ± 7.2	29.4 ± 2.6	3.4 ± 0.7
33.87 ± 0.50	28.1 ± 2.9	117.5 ± 10.6	88.7 ± 8.0	33.9 ± 3.1	4.7 ± 0.8
32.40 ± 0.53	14.3 ± 2.9	123.0 ± 11.2	89.3 ± 8.1	35.9 ± 3.2	4.9 ± 0.9
30.88 ± 0.57	6.4 ± 2.1	128.7 ± 11.6	84.9 ± 7.9	36.1 ± 3.2	4.7 ± 0.6
29.29 ± 0.61	6.0 ± 0.8	126.4 ± 11.4	81.5 ± 10.0	32.0 ± 2.9	4.3 ± 0.6
26.85 ± 0.65	3.4 ± 3.7	110.7 ± 10.3	56.2 ± 5.2	24.9 ± 2.6	3.4 ± 0.5
25.07 ± 0.69	0.71 ± 0.07	116.9 ± 10.6	47.4 ± 4.2	20.9 ± 2.0	2.7 ± 0.4
23.18 ± 0.75		65.4 ± 6.4		12.9 ± 1.3	1.4 ± 0.3
20.21 ± 0.82		9.7 ± 0.9	4.8 ± 0.5	3.91 ± 0.38	0.3 ± 0.09
19.68 ± 0.31				1.86 ± 0.24	
18.66 ± 0.32				1.77 ± 0.27	
17.60 ± 0.33				1.43 ± 0.28	
16.85 ± 0.90		2.2 ± 0.2	0.2 ± 0.05	1.52 ± 0.20	
16.38 ± 0.35				1.58 ± 0.27	
15.21 ± 0.36				0.85 ± 0.15	
14.43 ± 0.37				0.56 ± 0.15	
12.91 ± 0.98		0.2 ± 0.02		0.46 ± 0.05	

4.4. Production of Ga radionuclides

Bombarding natural germanium by alpha particles Ga isotopes can be produced by emission of 3 protons and additional neutrons, often including an α-cluster. Considering only the reaction Q-values at 52 MeV bombarding energy Ga isotopes can be produced with mass numbers from 65 to 77. In principle the decay parameters of the possible Ga radionuclides and the experimental conditions would have made it possible to deduce cross sections for production of the $^{66,67,72,73}Ga$ isotopes. However, due to the very thin targets, the low reaction cross section and/or the interferences of the gamma-lines the evaluated net counts were statistically non-significant and burdened with high uncertainty. Therefore, no reliable cross sections values were deduced for the Ga isotopes.

5. Thick target yields

The deduced experimental cross section data points were approximated by a cubic spline fit to provide a continuous curve for the excitation functions of the investigated reaction products. Using the fitted curves physical thick target yields were calculated for each process. The calculated physical thick target yields are presented in Fig. 11 and 12 together with the available experimental yield data. Experimental thick target yields are available in the literature for production of ^{72}Se [27], ^{73}Se [28], [29], ^{75}Se [27], ^{72}As [29] and ^{74}As [30],in the investigated energy range.

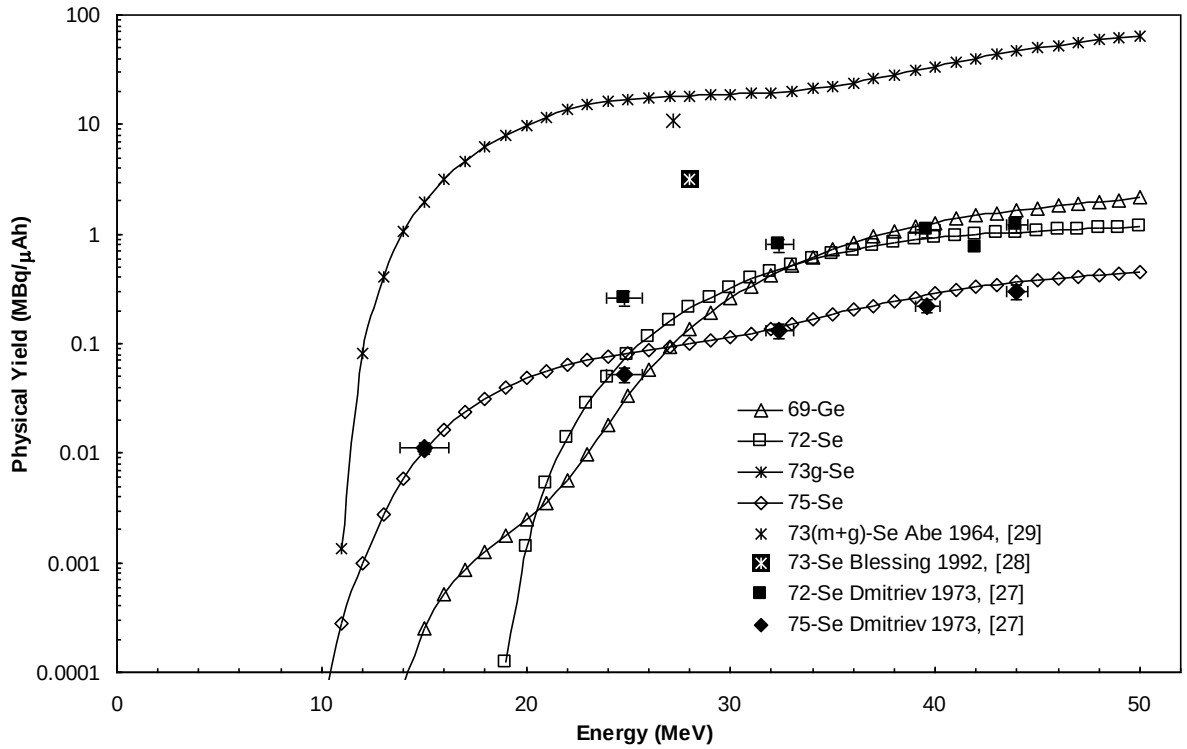

Figure 11. Calculated physical thick target yields for production of ^{72,73,75}Se and ^{69}Ge based on the newly measured cross section data in comparison with the available experimental yield data.

There are two experimental yield data points for production of $^{73m+g}$Se at E_α = 27.2 MeV by Abe et al. [29] and at E_α = 28 MeV by Blessing et al. [28] equal to 10.7 and 3.15 MBq/μAh, respectively. The calculated physical yields at both energy points are much higher, being 18.0 MBq/μAh and 18.2 MBq/μAh at E_α = 27.2 MeV and E_α = 28 MeV particle energies, respectively. The too low yield published by Blessing et al. [28] can be explained as the reported value is a batch yield on a Cu_3Ge target material and is affected by the chemical yield of the separation process. The value published by Abe et al. is a normalized EOB activity, which should be lower than the physical yield for the $T_{½}$ = 7.15 h half-life ^{73}Se radioisotope.

The experimental physical yields presented by Dmitriev et al. [30] in the E_α = 15–44 MeV energy window are in good agreement for production of ^{75}Se, but their experimental physical yields for production of ^{72}Se are too high. The experimental data may contain contribution from decay of interfering radionuclides.

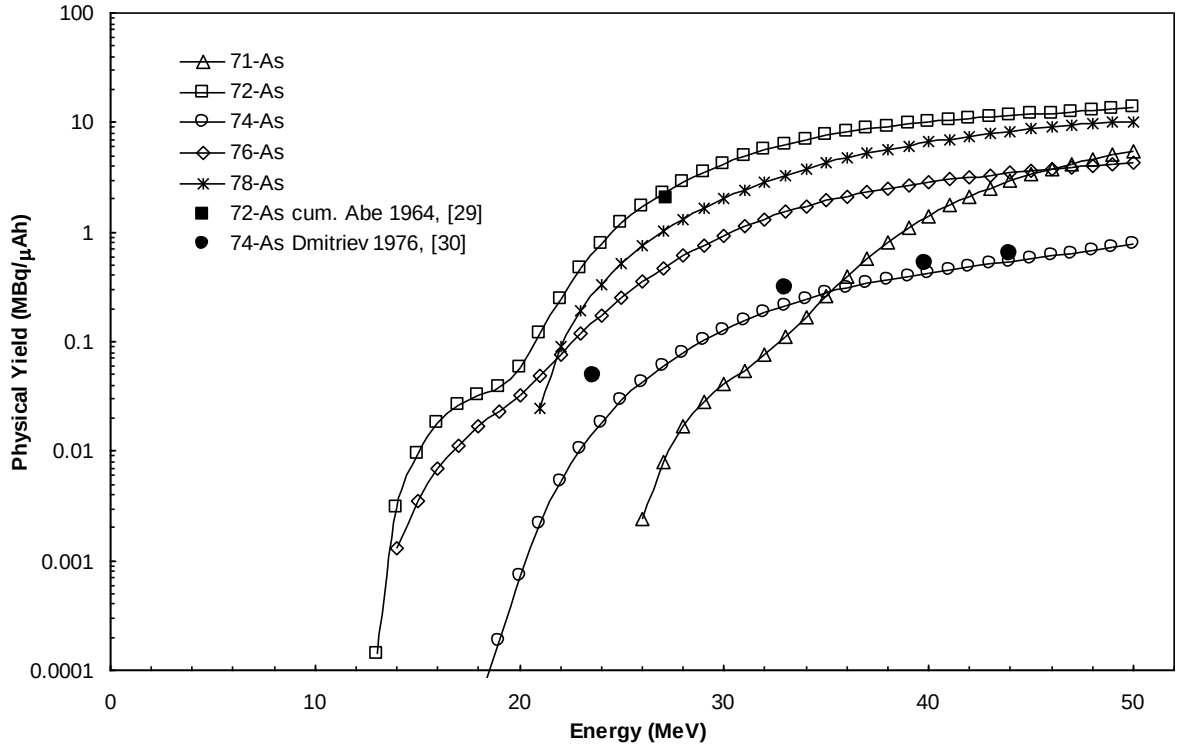

Figure 12. Calculated physical thick target yields for production of ^{71,72,74,76,78}As based on the newly measured cross section data in comparison with the available experimental yield data.

The value presented at a single E_α = 27.2 MeV energy point by Abe et al. [29] for production of ^{72}As is a normalized EOB activity which should be lower than the physical yield deduced from the newly measured cross section. The experimental physical yields published by the Dmitriev's group [30] for production of ^{74}As in the E_α = 23.6–44 MeV energy region are systematically higher than the calculated yields. Due to limited information about the experimental conditions in [30], no explanation was found for the discrepancy.

6. Conclusion

In this work activation cross sections were measured for 9 longer-lived products formed on ^{nat}Ge target by ^{4}He irradiation up to E_α = 51.25 MeV bombarding energy. Only few earlier measured data sets are available for the investigated processes. In most cases, only the data reported by Levkovskij [12] are available.

Regarding the production of Se isotopes on Ge target material with natural isotopic composition, no real production energy window can be defined in which one or more selenium isotopes can be produced without interference, due to the similar threshold energies of the possible reactions on different stable Ge isotopes. Production of ^{73}Se and ^{75}Se with minimal Se radio-isotopic contaminants is possible only on highly-enriched ^{70}Ge and ^{72}Ge target material respectively, up to about E_α = 20 and 30 MeV respectively. Depending on the enrichment level of the used target material, production of other Se radio isotopes in minor amount is unavoidable even in the applied energy windows.

Production of As radionuclides is possible in (α,pxn) reactions. The threshold energy of the (α,p) reactions is relatively low. Therefore, in principle, production of ^{73}As, ^{76}As, ^{77}As and ^{79}As with minimal As radioisotopic contaminants is possible on ^{70}Ge, ^{73}Ge, ^{74}Ge and ^{76}Ge

highly-enriched target material respectively, but due to the low cross section of the reactions the production is not feasible in the E_α = 5–15 MeV energy window. At higher bombarding energies direct and decay production of additional arsenic radionuclides is unavoidable. Only the longer-lived isotopes such as ^{75}Se or ^{73}As can be produced in relatively clean form by letting the short-lived contaminating radionuclides decay.
The prediction capability of the TALYS theoretical code is in general not so good. The investigated processes are combination of different reactions on the stable isotopes of Ge. The calculated results are combination of those individual reactions. The TALYS calculation result is not systematic, for example, the high energy part of the excitation function is too high for production of ^{73}Se, while the high energy part of the excitation function is too low for production of ^{75}Se. Both large under- and overestimations of the contributing reactions by the TALYS code can be found among the investigated processes. It may indicate problems of modelling the emission of multiple particles in the outgoing channel. Comparing the two latest results of the TALYS code (TENDL2014 and TENDL2015) no much improvement can be seen. Our experimental data can contribute to further development of the theoretical model and improve the prediction capabilities of the implemented computer code.

Acknowledgements

This work was carried out in the frame of the HAS-JSPS (Hungary–Japan) bilateral exchange agreement. The work was partly performed at the RI Beam Factory operated by the RIKEN Nishina Center and CNS, University of Tokyo. The authors acknowledge the support from the respective institutions in providing technical support and use of experimental facilities. (Contract No.: NKM-89/2014).

References

1 I. Spahn, G.F. Steyn, F.M. Nortier, H.H. Coenen, S.M. Qaim; *Excitation functions of ^{nat}Ge(p,xn)^{71,72,73,74}As reactions up to 100 MeV with a focus on the production of ^{72}As for medical and ^{73}As for environmental studies,* Applied Radiation and Isotopes 65 (2007) 1057

2 M. Jennewein, S.M. Qaim, P.V. Kulkarni, R.P. Mason, A. Hermanne, F. Rosch, *A no-carrier-added ^{72}Se/^{72}As generator based on solid phase extraction*. Radiochim. Acta 93(2005)579.

3 M. Jennewein, S.M. Qaim, A. Hermanne, M. Jahn, E. Tsyganov, N. Slavine, S. Seliounine, P.A. Antich, P.V. Kulkarni, P.E. Thorpe, R.P. Mason, F. Roch, *A new method for radiochemical separation of arsenic from germanium oxide.* Int. J. Appl. Radiat. Isot.63(2005)343.

4 S. Takács, M.P. Takács, A. Hermanne, F.Tárkányi, R. Adam-Rebeles: *Excitation functions of longer-lived radionuclides formed by deuteron irradiation of germanium.* Nucl. Inst. and Meth. B: 336(2014)81-95.

5 K. Otozai, S. Kuze, H.Okamura, A. Mito, T. Nishi, I. Fujiwara, *Excitation functions for deuterium-induced reactions,* Nucl. Phys. A 107(1968)427

6 W.Weirauch, W.D.Schmidt-Ott, *Search for As-74-m;* Zeitschrift fuer Physik 222(1969)474

7 S. Amiel, *Reactions of Alpha Particles with Germanium-70 and Zinc-70*, Phys. Rev. 116(1959)415-417, EXFOR:P0074

8 M. Guillaume, R.M. Lambrecht and A.P. Wolf, *Cyclotron Isotopes and Radio-pharmaceuticals -XXVII. ^{73}Se,* J. Appl. Radiat. Isot.29(1978)411-417, EXFOR:B0152

9 A. Calboreanu, O. Salagean, C. Pencea, K.W. Zimmer, a. Ciocanel, *Formation and decay of the compound nucleaus in alpha inducedreaction on Ge-70,* Revue Roumaine de Physique, 32(1987)725

10 S.M.Qaim, A.Mushtaq, M.Uhl, *Isomeric cross section ratio for the formation of Se-73m,g in various nuclear processes.,* Phys. Rev/C 38(1988)645

11 A.Mushtaq,S.M.Qaim, *Excitation functions of alpha- and ^{3}He-particle induced nuclear reactions on natural germanium: evaluation of production routes for ^{73}Se* , Radiochimica Acta 50(1990)27

12 V.N. Levkovskij :*Middle mass nuclides (A=40–100) activation cross-sections by medium energy (E=10–50 MeV) protons and alpha particles (experiment and systematics)*, Intervesi, Moscow, 1991.

13 M. Berglund and M. E. Wieser, *Isotopic compositions of the elements 2009 (IUPAC Technical Report),* Pure Appl. Chem., Vol. 83, No. 2, pp. 397–410, 2011

14 B. Ballard, F.M. Nortier, E.R. Birnbaum, K.D. John, D.R. Phillips and M.E. Fassbender; *Radioarsenic from a Portable 72Se/72As Generator: A Current Perspective,* Current Radiopharmaceuticals,5 (2012) 264-270

15 L. Brindley, *Arsenic enhances cancer imaging,*ChemistryWorld, 2008, March, URL: http://www.rsc.org/chemistryworld/News/2008/March/05030801.asp.

16 R. M. Santos Augusto, L. Buehler, Z. Lawson, S. Marzari, M. Stachura, T. Stora, and CERN-MEDICIS collaboration; *CERN-MEDICIS (Medical Isotopes Collected from ISOLDE): A New Facility,* Appl. Sci. 4 (2014) 265-281; doi:10.3390/app4020265

17 M. Fassbender, W.Taylor, D.Vieira, M.Nortier, H.Bach, K.John; *Proton beam simulation with MCNPX/CINDER'90:Germanium metal activation estimates below 30 MeV relevant to the bulk production of arsenic radioisotopes,* Applied Radiation and Isotopes 70 (2012) 72–75

18 M. Neves, A. Kling, R.M. Lambrecht; *Radionuclide production for therapeutic radiopharmaceuticals*, Applied Radiation and Isotopes 57 (2002) 657–664

19 T. Watanabe, M. Fujimaki, N. Fukunishi, H. Imao, O. Kamigaito, M. Kase, M. Komiyama, N. Sakamoto, K. Suda, M. Wakasugi, K. Yamada, Beam Energy and Longitudinal Beam Profile Measurement System at RIBF, in: 5th International Particle Accelerator Conference (IPAC2014), Jacow, Dresden, Germany, 2014, pp. 3566.

20 T. Watanabe, in: 12th Annual Meeting of Particle Accelerator Society of Japan, PASJ, 2015, pp. 1198.

21 IAEA-TECDOC-1211, *Charged particle cross section database for medical radioisotope production. Beam Monitor Reactions (Chapter 4),* IAEA-TECDOC-1211, Vienna, 2001, URL: http://www-nds.iaea.org/medical/monitor_reactions.html (updated in March 2007)

22 G. Székely, *FGM — A flexible gamma-spectrum analysis program for a small computer*, Comp. Phys. Comm. 34 (1985) 313.

23 H.H. Andersen, J.F. Ziegler, 1977. *Hydrogen Stopping powers and ranges in all elements*, Volume 3 of the Stopping and ranges of ions in matter, Pergamon Press, ISBN 0-08-021605-6.

24 Nuclear structure and decay data on-line library, Nudat 2.6, National Nuclear Data Center, Brookhaven National Laboratory, USA
URL: http://www.nndc.bnl.gov/nudat2/

25 Q-value Calculator (QCalc), http://www.nndc.bnl.gov/qcalc/

26 A. J. Koning., D. Rochman, et al. *"TENDL-2015: (release date: 18 January 2016)"* Database available from:
URL: https://tendl.web.psi.ch/tendl_2015/alpha_html/Ge/AlphaGe.html

27 P.P. Dmitriev, G.A. Molin, I.O. Konstantinov, N.N. Krasnov and M.V. Panarii, *Yields of ^{72}Se and ^{75}Se in nuclear reactionswith protons, deuterons and a-particles,* Sovjet Atomic

Energy, 34(1973)499, (Translated from Atomnaya Energiya, Vol. 34, No. 5, pp. 405-406, May, 1973), EXFOR: A0022

28 G. Blessing, N. Lavi and S.M. Qaim, *Production of ^{73}Se via the ^{70}Ge(α,n)-Process Using High Current Target Materials,* Appl. Radiat. Isot. Vol. 43, No. 3, pp. 455-461, 1992, EXFOR: D0085

29 K. Abe, A. Iizuka, A. Hasegawa and S. Morozumi, *Induced radioactivity of component materials by 16-MeV protons and 30-MeV alpha particles*, Journal of Nuclear Materials 122 & 123(1984)972, EXFOR:E1964

30 P.P Dmitriev and G.A. Molin, *The Yields of As-73 and As-74 in nuclear reactions with protons, deuterons and alpha particles,* Sovjet Atomic Energy, 41(1976)657, (Translated from Atomnaya Energiya, Vol. 41(1976)48), EXFOR: A0006